The Spectrometer/Telescope for Imaging X-rays on-board Solar Orbiter: from photon to electron visibilities.

MIDAgroup

Università di Genova
DIMA | Dipartimento di Matematica

Anna Volpara

Potsdam, AIP
September, 2023

Outline

1. From photon to electron visibilities
2. Visibility inversion algorithm
3. Application to STIX visibilities
4. Conclusions and future works

Outline

1. **From photon to electron visibilities**
2. Visibility inversion algorithm
3. Application to STIX visibilities
4. Conclusions and future works

From photon to electron visibilities

Photon visibilities:

$$V(u, v; \epsilon) = \mathcal{F}(I(x, y; \epsilon)) = \int\int I(x, y; \epsilon) e^{2\pi i (xu + yv)}\, dx\, dy \qquad (1)$$

From photon to electron visibilities

Photon visibilities:

$$V(u,v;\epsilon) = \mathcal{F}(I(x,y;\epsilon)) = \int\int I(x,y;\epsilon)e^{2\pi i(xu+yv)}\,dx\,dy \tag{1}$$

Intensity of the X-ray photon flux emitted from (x, y) on the Sun

From photon to electron visibilities

Photon visibilities:

$$V(u, v; \epsilon) = \mathcal{F}(I(x, y; \epsilon)) = \int \int I(x, y; \epsilon) e^{2\pi i (xu + yv)} \, dx \, dy \tag{1}$$

The Fourier Transform

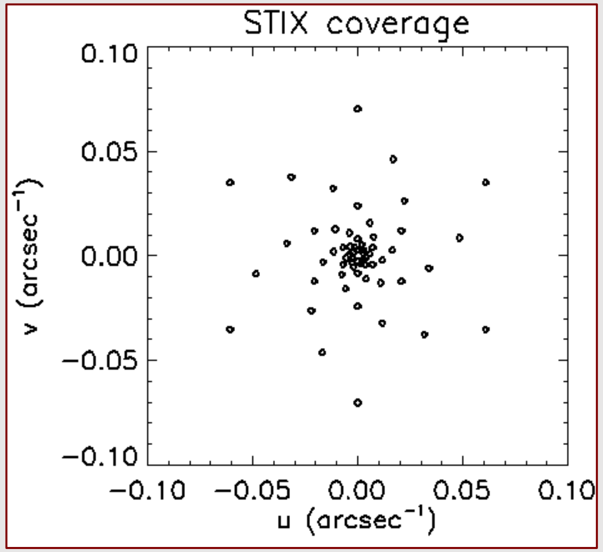

Figure: (u, v) frequencies sampled by STIX sub-collimators.

From photon to electron visibilities

Photon visibilities:

$$V(u, v; \epsilon) = \mathcal{F}(I(x, y; \epsilon)) = \int\int I(x, y; \epsilon) e^{2\pi i (xu + yv)}\, dx\, dy \qquad (1)$$

Array containing the N_V complex values of the visibilities measured by STIX

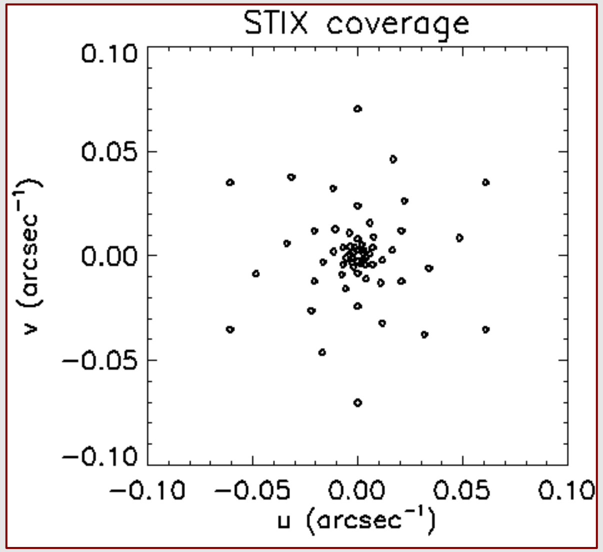

Figure: (u, v) frequencies sampled by STIX sub-collimators.

From photon to electron visibilities

Photon visibilities:

$$V(u, v; \epsilon) = \mathcal{F}(I(x, y; \epsilon)) = \int\int I(x, y; \epsilon) e^{2\pi i(xu+yv)}\, dx\, dy \tag{1}$$

Electron visibilities:

$$W(u, v; E) = \frac{a}{4\pi R^2} \int\int N(x, y) \bar{F}(x, y; E) e^{2\pi i(xu+yv)}\, dx\, dy \tag{2}$$

Prato et al., *A Regularized Visibility-Based Approach to Astronomical Imaging Spectroscopy*, SIAM Journal on Imaging Sciences, (2009)

Piana et al., *Electron flux spectral imaging of solar flares through regularized analysis of hard x-ray source visibilities,* The Astrophysical Journal, (2007)

From photon to electron visibilities

Photon visibilities:

$$V(u,v;\epsilon) = \mathcal{F}(I(x,y;\epsilon)) = \int\int I(x,y;\epsilon)e^{2\pi i(xu+yv)}\,dx\,dy \tag{1}$$

Electron visibilities:

$$W(u,v;E) = \frac{a}{4\pi R^2}\int\int N(x,y)\bar{F}(x,y;E)e^{2\pi i(xu+yv)}\,dx\,dy \tag{2}$$

Prato et al., *A Regularized Visibility-Based Approach to Astronomical Imaging Spectroscopy*, SIAM Journal on Imaging Sciences, (2009)

Piana et al., *Electron flux spectral imaging of solar flares through regularized analysis of hard x-ray source visibilities,* The Astrophysical Journal, (2007)

From photon to electron visibilities

Photon visibilities:

$$V(u,v;\epsilon) = \mathcal{F}(I(x,y;\epsilon)) = \int\int I(x,y;\epsilon) e^{2\pi i(xu+yv)}\, dx\, dy \qquad (1)$$

Electron visibilities:

$$W(u,v;E) = \frac{a}{4\pi R^2}\int\int N(x,y)\bar{F}(x,y;E) e^{2\pi i(xu+yv)}\, dx\, dy \qquad (2)$$

$$N(x,y) = \int_0^{\ell(x,y)} n(x,y,z)\, dz$$

$n(x,y,z)$ is the local density of target particles along the line-of-sight depth $\ell(x,y)$

$$\bar{F}(x,y;E) = \frac{1}{N(x,y)}\int_0^{\ell(x,y)} n(x,y,z) F(x,y,z;E)\, dz$$

$F(x,y,z;E)$ is the differential electron flux spectrum at the point (x,y,z)

Prato et al., *A Regularized Visibility-Based Approach to Astronomical Imaging Spectroscopy*, SIAM Journal on Imaging Sciences, (2009)

Piana et al., *Electron flux spectral imaging of solar flares through regularized analysis of hard x-ray source visibilities,* The Astrophysical Journal, (2007)

From photon to electron visibilities

Photon visibilities:

$$V(u,v;\epsilon) = \mathcal{F}(I(x,y;\epsilon)) = \int\int I(x,y;\epsilon)e^{2\pi i(xu+yv)}\,dx\,dy \tag{1}$$

Electron visibilities:

$$W(u,v;E) = \frac{a}{4\pi R^2}\int\int N(x,y)\bar{F}(x,y;E)e^{2\pi i(xu+yv)}\,dx\,dy \tag{2}$$

Bremsstralhung equation for visibilities:

$$V(u,v;\epsilon) = \int_{\epsilon}^{\infty} W(u,v;E)Q(\epsilon,E)\,dE \tag{3}$$

Prato et al., *A Regularized Visibility-Based Approach to Astronomical Imaging Spectroscopy*, SIAM Journal on Imaging Sciences, (2009)

Piana et al., *Electron flux spectral imaging of solar flares through regularized analysis of hard x-ray source visibilities,* The Astrophysical Journal, (2007)

From photon to electron visibilities

Photon visibilities:

$$V(u,v;\epsilon) = \mathcal{F}(I(x,y;\epsilon)) = \int\int I(x,y;\epsilon)e^{2\pi i(xu+yv)}\,dx\,dy \tag{1}$$

Electron visibilities:

$$W(u,v;E) = \frac{a}{4\pi R^2}\int\int \boxed{N(x,y)\bar{F}(x,y;E)}e^{2\pi i(xu+yv)}\,dx\,dy \tag{2}$$

Bremsstralhung equation for visibilities:

$$V(u,v;\epsilon) = \int_{\epsilon}^{\infty} \boxed{W(u,v;E)}Q(\epsilon,E)\,dE \tag{3}$$

Prato et al., *A Regularized Visibility-Based Approach to Astronomical Imaging Spectroscopy*, SIAM Journal on Imaging Sciences, (2009)

Piana et al., *Electron flux spectral imaging of solar flares through regularized analysis of hard x-ray source visibilities,* The Astrophysical Journal, (2007)

Outline

1. From photon to electron visibilities
2. **Visibility inversion algorithm**
3. Application to STIX visibilities
4. Conclusions and future works

Visibility inversion algorithm - Photon visibilities

Photon visibilities

$$\begin{array}{c|c|}
 & \varepsilon_1 \\
\hline
(u_1, v_1) & V_{1,1} \\
(u_2, v_2) & V_{2,1} \\
\vdots & \vdots \\
(u_{N_V}, v_{N_V}) & V_{N_V,1} \\
\hline
\end{array}$$

Piana et al., *Electron flux spectral imaging of solar flares through regularized analysis of hard x-ray source visibilities,* The Astrophysical Journal, (2007)

Visibility inversion algorithm - Photon visibilities

Photon visibilities

$$
\begin{array}{c}
\\
(u_1, v_1) \\
(u_2, v_2) \\
\vdots \\
(u_{N_V}, v_{N_V})
\end{array}
\begin{array}{cccc}
\varepsilon_1 & \varepsilon_2 & \cdots\cdots & \varepsilon_N \\
\hline
\multicolumn{1}{|c}{V_{1,1}} & V_{1,2} & \cdots\cdots & \multicolumn{1}{c|}{V_{1,N}} \\
\multicolumn{1}{|c}{V_{2,1}} & V_{2,2} & \cdots\cdots & \multicolumn{1}{c|}{V_{2,N}} \\
\multicolumn{1}{|c}{\vdots} & \vdots & \ddots & \multicolumn{1}{c|}{\vdots} \\
\multicolumn{1}{|c}{V_{N_V,1}} & V_{N_V,2} & \cdots\cdots & \multicolumn{1}{c|}{V_{N_V,N}} \\
\hline
\end{array}
$$

Piana et al., *Electron flux spectral imaging of solar flares through regularized analysis of hard x-ray source visibilities,* The Astrophysical Journal, (2007)

Visibility inversion algorithm - Photon visibilities

Photon visibilities

$$
\begin{array}{c|cccc|}
 & \varepsilon_1 & \varepsilon_2 & \cdots & \varepsilon_N \\
\hline
(u_1, v_1) & V_{1,1} & V_{1,2} & \cdots & V_{1,N} \\
(u_2, v_2) & V_{2,1} & V_{2,2} & \cdots & V_{2,N} \\
\vdots & \vdots & \vdots & \ddots & \vdots \\
(u_{N_V}, v_{N_V}) & V_{N_V,1} & V_{N_V,2} & \cdots & V_{N_V,N} \\
\hline
\end{array}
$$

Piana et al., *Electron flux spectral imaging of solar flares through regularized analysis of hard x-ray source visibilities,* The Astrophysical Journal, (2007)

Visibility inversion algorithm - Photon visibilities

Photon visibilities

$$
\begin{array}{c|cccc|}
 & \varepsilon_1 & \varepsilon_2 & \cdots\cdots & \varepsilon_N \\
\hline
(u_1, v_1) & V_{1,1} & V_{1,2} & \cdots\cdots & V_{1,N} \\
(u_2, v_2) & V_{2,1} & V_{2,2} & \cdots\cdots & V_{2,N} \\
\vdots & \vdots & \vdots & \ddots & \vdots \\
(u_{N_V}, v_{N_V}) & V_{N_V,1} & V_{N_V,2} & \cdots\cdots & V_{N_V,N} \\
\hline
\end{array}
$$

Solving image reconstruction problem via imaging methods.

May 7, 2021 – 18:51 UT

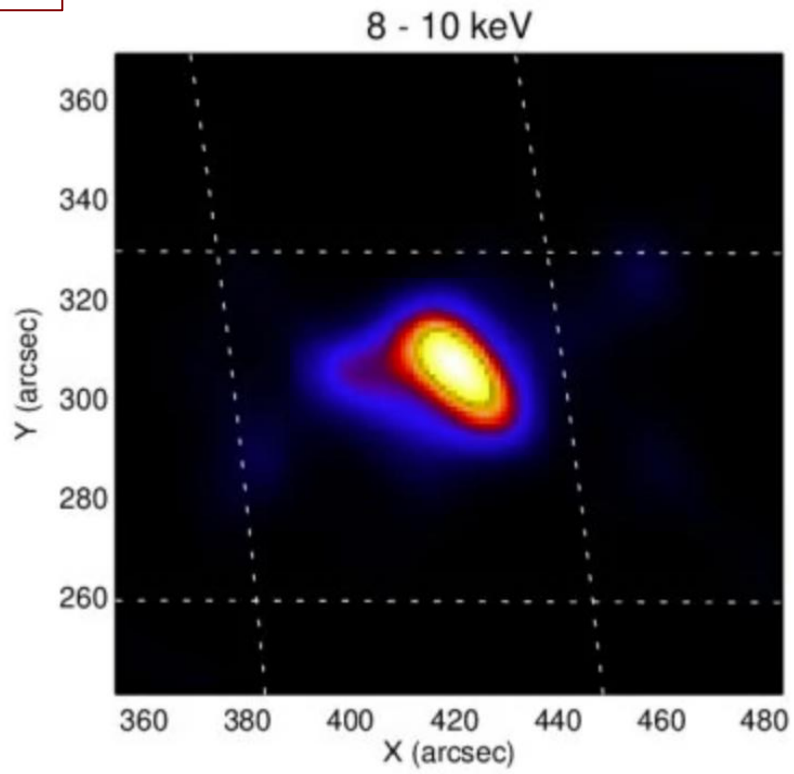

Figure: Reconstruction provided by MEM_GE, from **photon visibilities**.

Piana et al., *Electron flux spectral imaging of solar flares through regularized analysis of hard x-ray source visibilities,* The Astrophysical Journal, (2007)

Visibility inversion algorithm

Photon visibilities

$$
\begin{array}{c|cccc|}
 & \varepsilon_1 & \varepsilon_2 & \cdots\cdots & \varepsilon_N \\
\hline
(u_1, v_1) & V_{1,1} & V_{1,2} & \cdots\cdots & V_{1,N} \\
(u_2, v_2) & V_{2,1} & V_{2,2} & \cdots\cdots & V_{2,N} \\
\vdots & \vdots & \vdots & \ddots & \vdots \\
(u_{N_V}, v_{N_V}) & V_{N_V,1} & V_{N_V,2} & \cdots\cdots & V_{N_V,N} \\
\hline
\end{array}
$$

Piana et al., *Electron flux spectral imaging of solar flares through regularized analysis of hard x-ray source visibilities,* The Astrophysical Journal, (2007)

Prato et al., *A Regularized Visibility-Based Approach to Astronomical Imaging Spectroscopy*, SIAM Journal on Imaging Sciences, (2009)

Visibility inversion algorithm

Spectral inversion via regularized inversion technique (Tikhonov)

Photon visibilities

$$\begin{array}{c|cccc|} & \varepsilon_1 & \varepsilon_2 & \cdots\cdots & \varepsilon_N \\ \hline (u_1,v_1) & V_{1,1} & V_{1,2} & \cdots\cdots & V_{1,N} \\ (u_2,v_2) & V_{2,1} & V_{2,2} & \cdots\cdots & V_{2,N} \\ \vdots & \vdots & \vdots & \ddots & \vdots \\ (u_{N_V},v_{N_V}) & V_{N_V,1} & V_{N_V,2} & \cdots\cdots & V_{N_V,N} \\ \hline \end{array}$$

Electron visibilities

$$\begin{array}{c|cccc|} & E_1 & E_2 & \cdots\cdots\cdots & E_M \\ \hline (u_1,v_1) & W_{1,1} & W_{1,2} & \cdots\cdots\cdots & W_{1,M} \\ (u_2,v_2) & & & & \\ \vdots & & & & \\ u_{N_V},v_{N_V}) & & & & \\ \hline \end{array}$$

Piana et al., *Electron flux spectral imaging of solar flares through regularized analysis of hard x-ray source visibilities,* The Astrophysical Journal, (2007)
Prato et al., *A Regularized Visibility-Based Approach to Astronomical Imaging Spectroscopy*, SIAM Journal on Imaging Sciences, (2009)

Visibility inversion algorithm

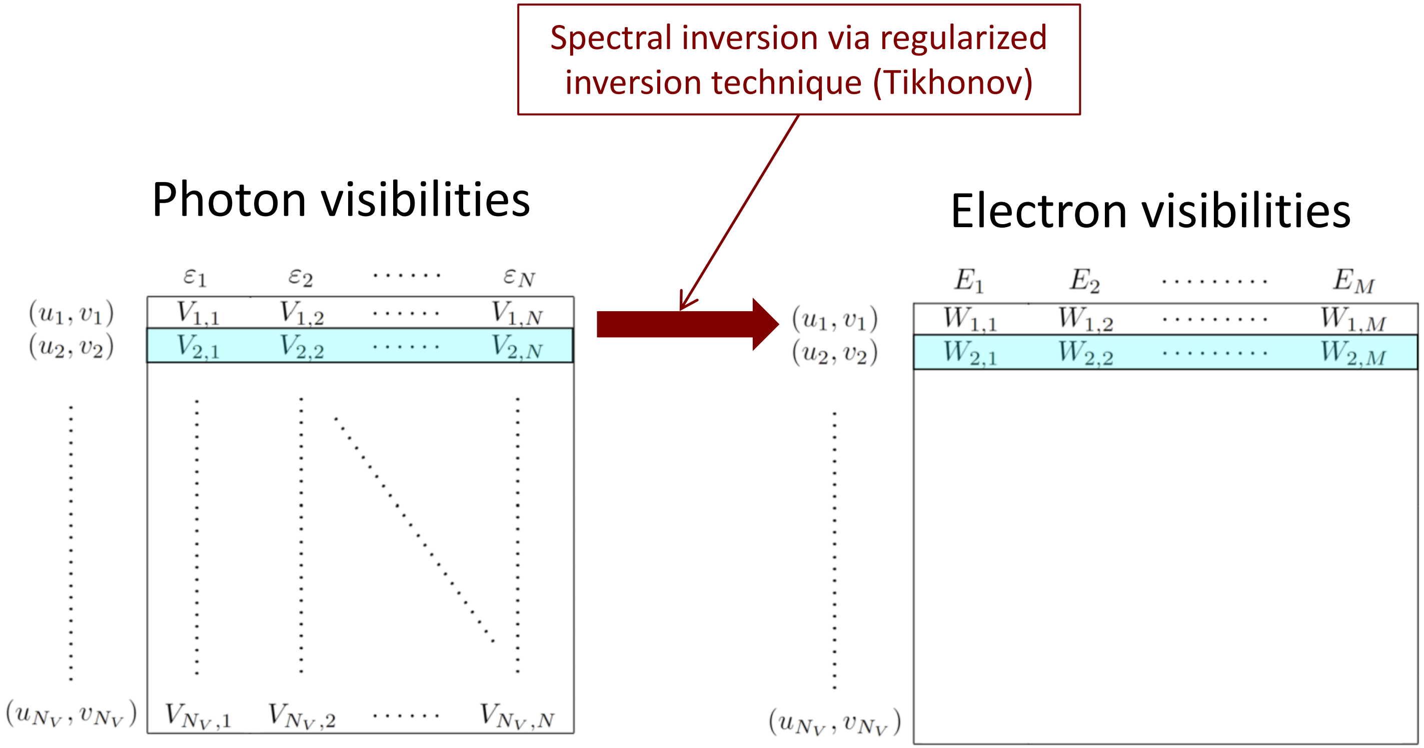

Piana et al., *Electron flux spectral imaging of solar flares through regularized analysis of hard x-ray source visibilities,* The Astrophysical Journal, (2007)
Prato et al., *A Regularized Visibility-Based Approach to Astronomical Imaging Spectroscopy*, SIAM Journal on Imaging Sciences, (2009)

Visibility inversion algorithm

Spectral inversion via regularized inversion technique (Tikhonov)

Photon visibilities

$$
\begin{array}{c|cccc|}
 & \varepsilon_1 & \varepsilon_2 & \cdots\cdots & \varepsilon_N \\
\hline
(u_1, v_1) & V_{1,1} & V_{1,2} & \cdots\cdots & V_{1,N} \\
(u_2, v_2) & V_{2,1} & V_{2,2} & \cdots\cdots & V_{2,N} \\
\vdots & \vdots & \vdots & \ddots & \vdots \\
(u_{N_V}, v_{N_V}) & V_{N_V,1} & V_{N_V,2} & \cdots\cdots & V_{N_V,N} \\
\hline
\end{array}
\quad \Longrightarrow
$$

Electron visibilities

$$
\begin{array}{c|cccc|}
 & E_1 & E_2 & \cdots\cdots\cdots & E_M \\
\hline
(u_1, v_1) & W_{1,1} & W_{1,2} & \cdots\cdots\cdots & W_{1,M} \\
(u_2, v_2) & W_{2,1} & W_{2,2} & \cdots\cdots\cdots & W_{2,M} \\
\vdots & \vdots & \vdots & \ddots & \vdots \\
(u_{N_V}, v_{N_V}) & W_{N_V,1} & W_{N_V,2} & \cdots\cdots\cdots & W_{N_V,M} \\
\hline
\end{array}
$$

Piana et al., *Electron flux spectral imaging of solar flares through regularized analysis of hard x-ray source visibilities,* The Astrophysical Journal, (2007)
Prato et al., *A Regularized Visibility-Based Approach to Astronomical Imaging Spectroscopy*, SIAM Journal on Imaging Sciences, (2009)

Visibility inversion algorithm

Spectral inversion via regularized inversion technique (Tikhonov)

Solving image reconstruction problem via imaging methods.

Photon visibilities

$$\begin{array}{c|cccc|} & \varepsilon_1 & \varepsilon_2 & \cdots & \varepsilon_N \\ \hline (u_1, v_1) & V_{1,1} & V_{1,2} & \cdots & V_{1,N} \\ (u_2, v_2) & V_{2,1} & V_{2,2} & \cdots & V_{2,N} \\ \vdots & \vdots & \vdots & \ddots & \vdots \\ (u_{N_V}, v_{N_V}) & V_{N_V,1} & V_{N_V,2} & \cdots & V_{N_V,N} \\ \hline \end{array}$$

Electron visibilities

$$\begin{array}{c|c|ccc|} & E_1 & E_2 & \cdots & E_M \\ \hline (u_1, v_1) & W_{1,1} & W_{1,2} & \cdots & W_{1,M} \\ (u_2, v_2) & W_{2,1} & W_{2,2} & \cdots & W_{2,M} \\ \vdots & \vdots & \vdots & \ddots & \vdots \\ (u_{N_V}, v_{N_V}) & W_{N_V,1} & W_{N_V,2} & \cdots & W_{N_V,M} \\ \hline \end{array}$$

May 7, 2021 – 18:51 UT

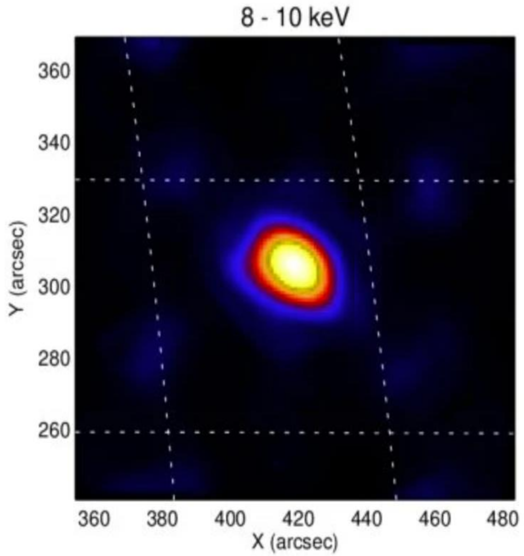

Figure: Reconstruction provided by MEM_GE, from **electron visibilities**.

Piana et al., *Electron flux spectral imaging of solar flares through regularized analysis of hard x-ray source visibilities,* The Astrophysical Journal, (2007)
Prato et al., *A Regularized Visibility-Based Approach to Astronomical Imaging Spectroscopy*, SIAM Journal on Imaging Sciences, (2009)

Outline

1. From photon to electron visibilities
2. Visibility inversion algorithm
3. **Application to STIX visibilities**
4. Conclusions and future works

September 29, 2022

Photon images

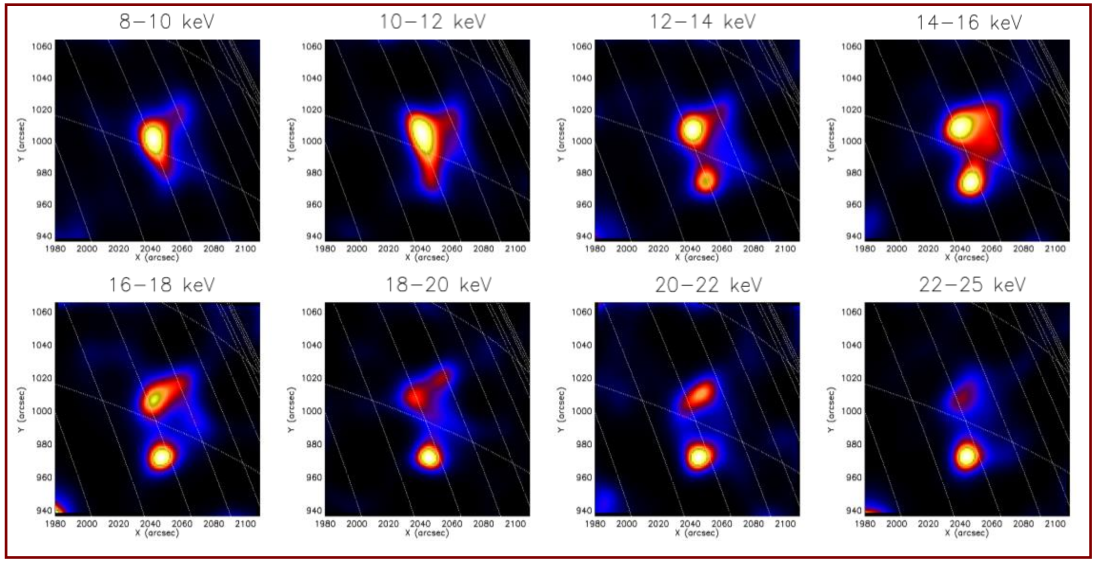

Electron flux images

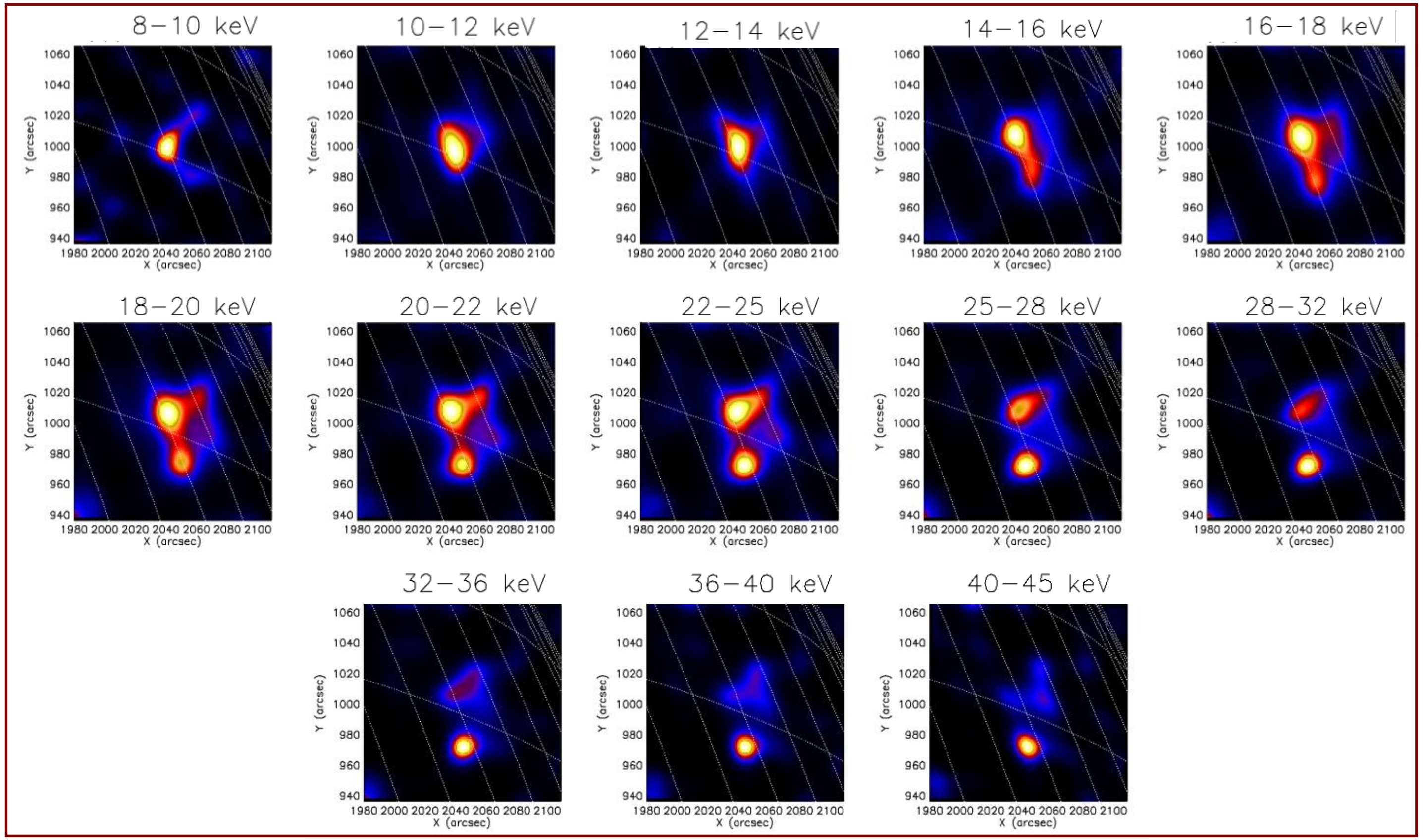

Figure: Photon images (*left panels*) compared with the electron flux images corresponding to the regularized electron visibilities (*right panels*) for the energy intervals shown. The maps are produced using the MEM-GE algorithm.

September 29, 2022

Photon images

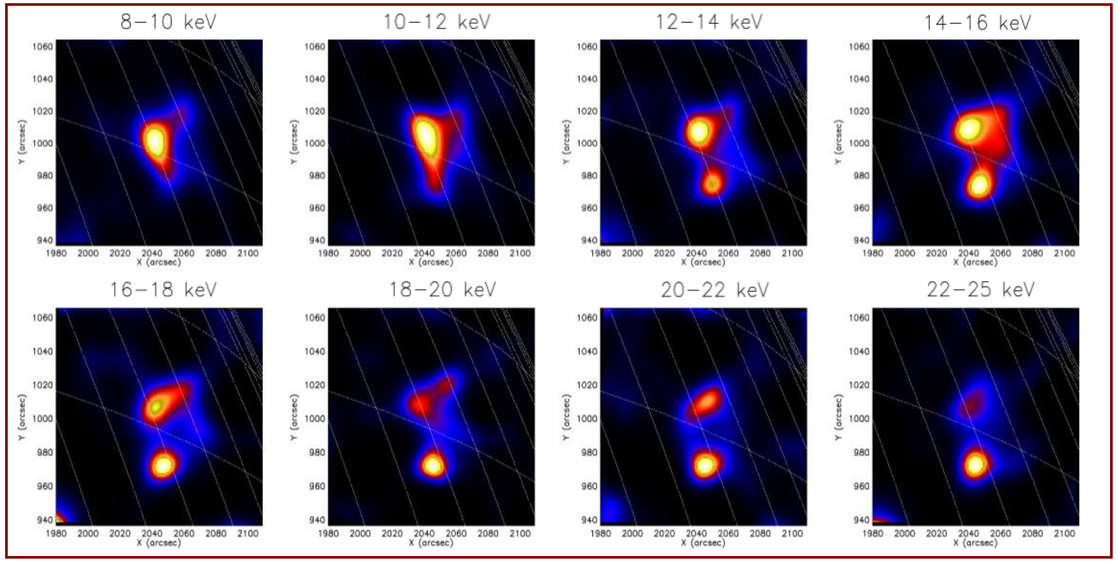

Regularized photon images

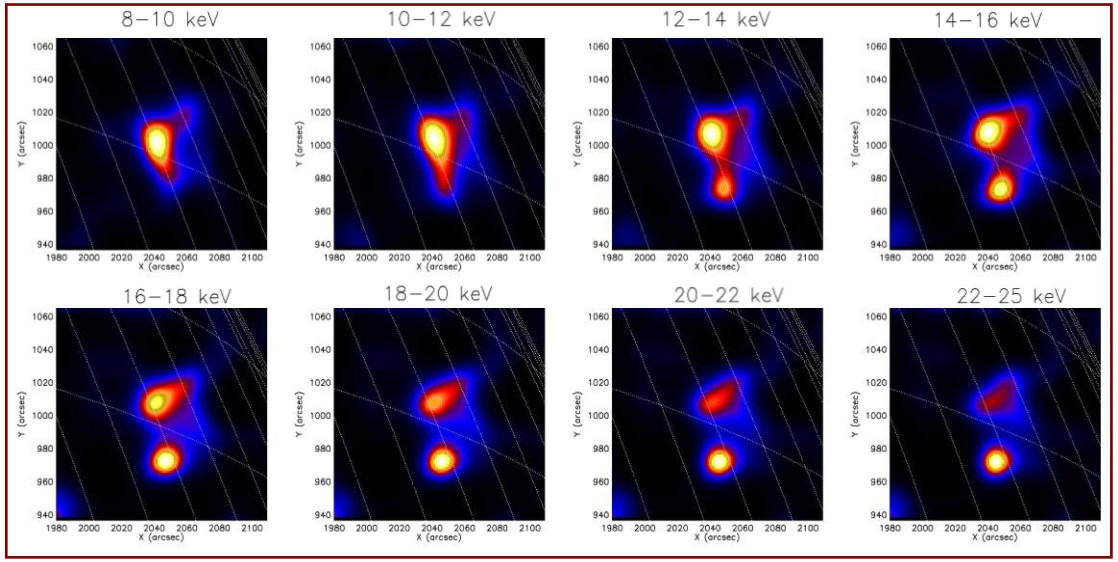

Figure: Photon images (*left panels*) for the energy intervals shown, compared with the regularized photon maps (*right panels*) in the same energy range. The maps are produced using the MEM-GE algorithm.

September 29, 2022

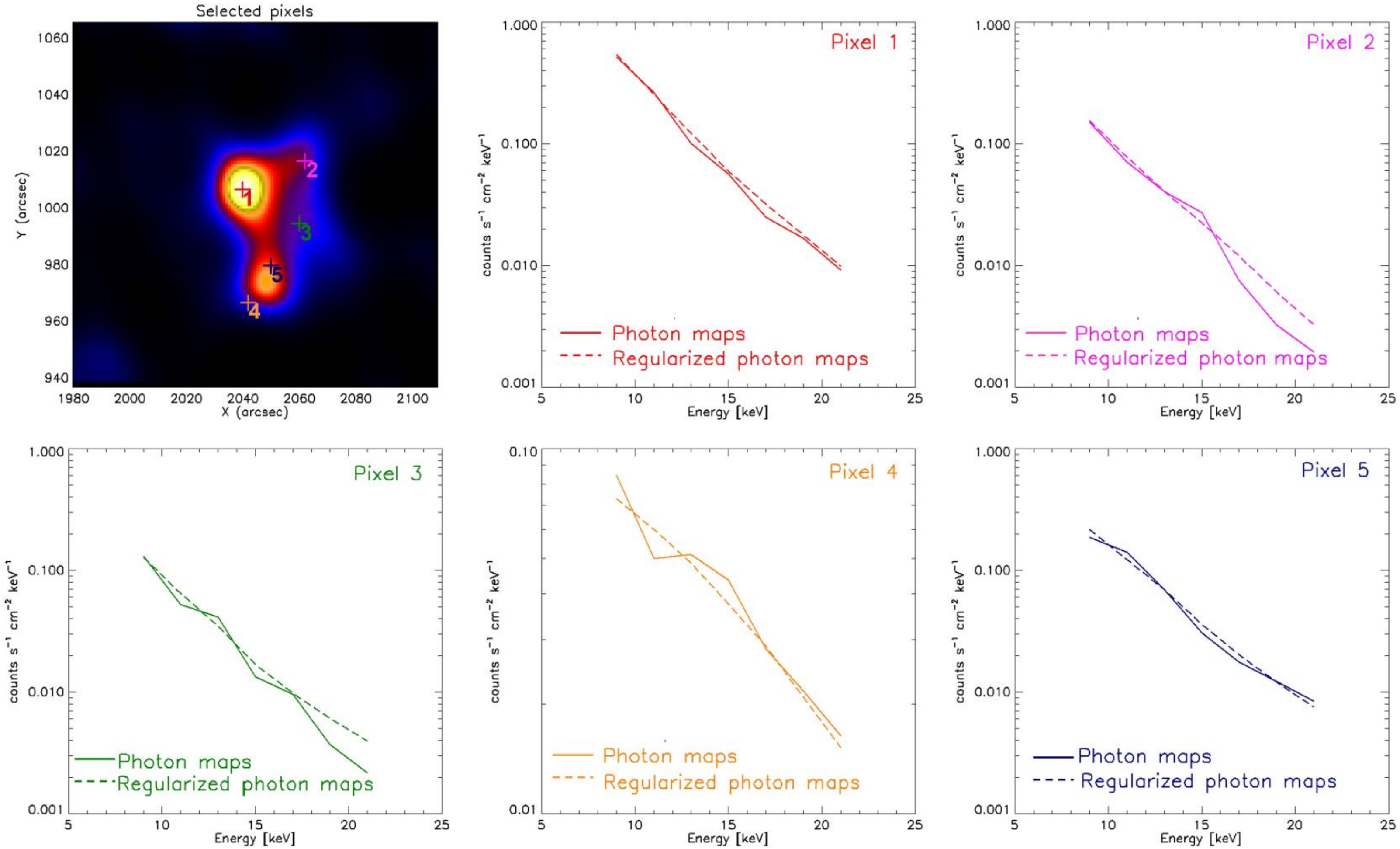

Figure: Pixel-wise spectrum obtained from photon maps and regularized photon maps. *Top left panel*: selected pixels are indicated with colored crosses. The other panels show the pixel-wise spectrum obtained from photon maps (*solid line*) and regularized photon maps (*dotted line*). The pixels selected in the top left panel and their respective spectra are indicated with the same colour. Plots are logarithmic scaled on the y-axis.

September 29, 2022

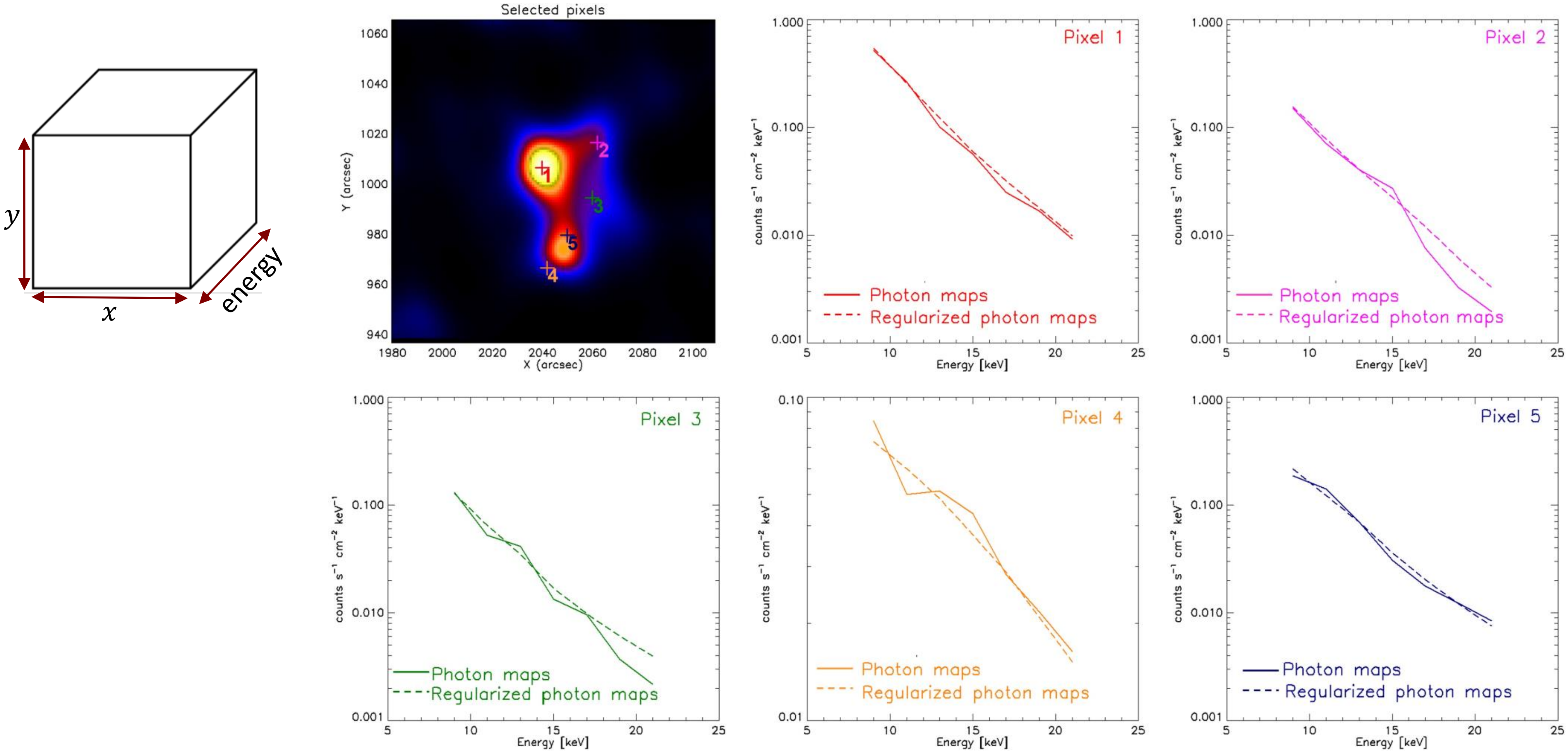

Figure: Pixel-wise spectrum obtained from photon maps and regularized photon maps. *Top left panel*: selected pixels are indicated with colored crosses. The other panels show the pixel-wise spectrum obtained from photon maps (*solid line*) and regularized photon maps (*dotted line*). The pixels selected in the top left panel and their respective spectra are indicated with the same colour. Plots are logarithmic scaled on the y-axis.

September 29, 2022

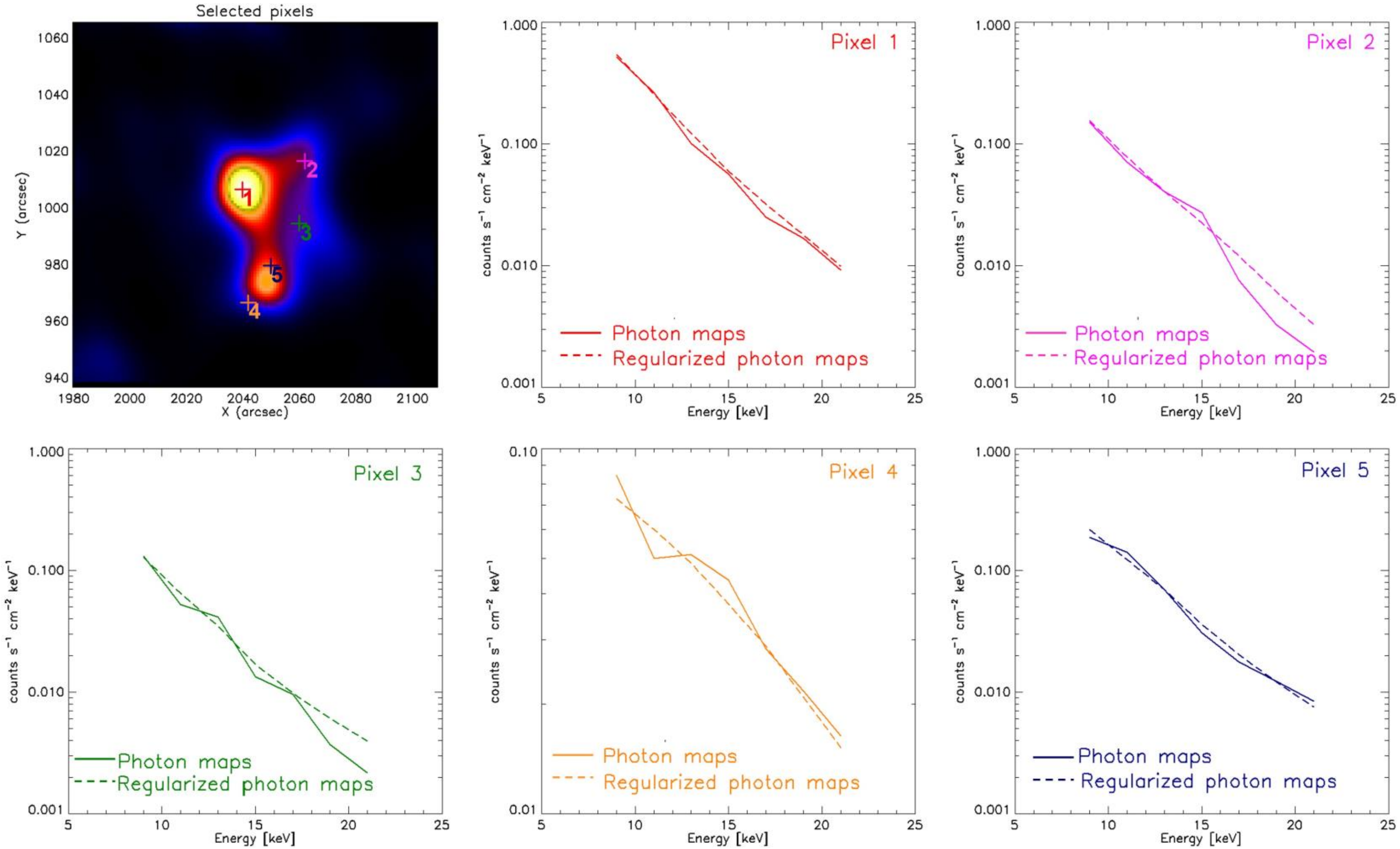

Figure: Pixel-wise spectrum obtained from photon maps and regularized photon maps. *Top left panel*: selected pixels are indicated with colored crosses. The other panels show the pixel-wise spectrum obtained from photon maps (*solid line*) and regularized photon maps (*dotted line*). The pixels selected in the top left panel and their respective spectra are indicated with the same colour. Plots are logarithmic scaled on the y-axis.

Validation

Event	OSPEX	electron maps	photon maps	regularized photon maps
May 08, 2021	$\gamma = 5.25$	$\delta = 4.53$	$\gamma = 4.94$	$\gamma = 5.50$
August 26, 2021	$\gamma = 5.47$	$\delta = 4.59$	$\gamma = 5.27$	$\gamma = 5.57$
January 20, 2022	$\gamma = 6.35$	$\delta = 4.91$	$\gamma = 6.25$	$\gamma = 6.36$
August 28, 2022	$\gamma = 6.94$	$\delta = 4.97$	$\gamma = 6.88$	$\gamma = 6.81$
September 29, 2022	$\gamma = 4.49$	$\delta = 3.68$	$\gamma = 4.24$	$\gamma = 4.42$

Table: Global spectral indices provided by OSPEX, electron maps, photon maps, and regularized photon maps.

Validation

Event	OSPEX	electron maps	photon maps	regularized photon maps
May 08, 2021	$\gamma = 5.25$	$\delta = 4.53$	$\gamma = 4.94$	$\gamma = 5.50$
August 26, 2021	$\gamma = 5.47$	$\delta = 4.59$	$\gamma = 5.27$	$\gamma = 5.57$
January 20, 2022	$\gamma = 6.35$	$\delta = 4.91$	$\gamma = 6.25$	$\gamma = 6.36$
August 28, 2022	$\gamma = 6.94$	$\delta = 4.97$	$\gamma = 6.88$	$\gamma = 6.81$
September 29, 2022	$\gamma = 4.49$	$\delta = 3.68$	$\gamma = 4.24$	$\gamma = 4.42$

Table: Global spectral indices provided by OSPEX, electron maps, photon maps, and regularized photon maps.

Validation

Event	OSPEX	electron maps	photon maps	regularized photon maps
May 08, 2021	$\gamma = 5.25$	$\delta = 4.53$	$\gamma = 4.94$	$\gamma = 5.50$
August 26, 2021	$\gamma = 5.47$	$\delta = 4.59$	$\gamma = 5.27$	$\gamma = 5.57$
January 20, 2022	$\gamma = 6.35$	$\delta = 4.91$	$\gamma = 6.25$	$\gamma = 6.36$
August 28, 2022	$\gamma = 6.94$	$\delta = 4.97$	$\gamma = 6.88$	$\gamma = 6.81$
September 29, 2022	$\gamma = 4.49$	$\delta = 3.68$	$\gamma = 4.24$	$\gamma = 4.42$

Table: Global spectral indices provided by OSPEX, electron maps, photon maps, and regularized photon maps.

STIX vs RHESSI

	STIX	RHESSI
Distance from the Sun	Variable	Fixed
Energy sampling	Non-uniform	Uniform
Gaps	provides its set of visibility values at all count energies → no (u, v) point gaps	gaps due to insufficient signal-to-noise as the visibility value in question → different energy bins have different number of samples

Table: Differences between STIX and RHESSI inversion software.

STIX vs RHESSI

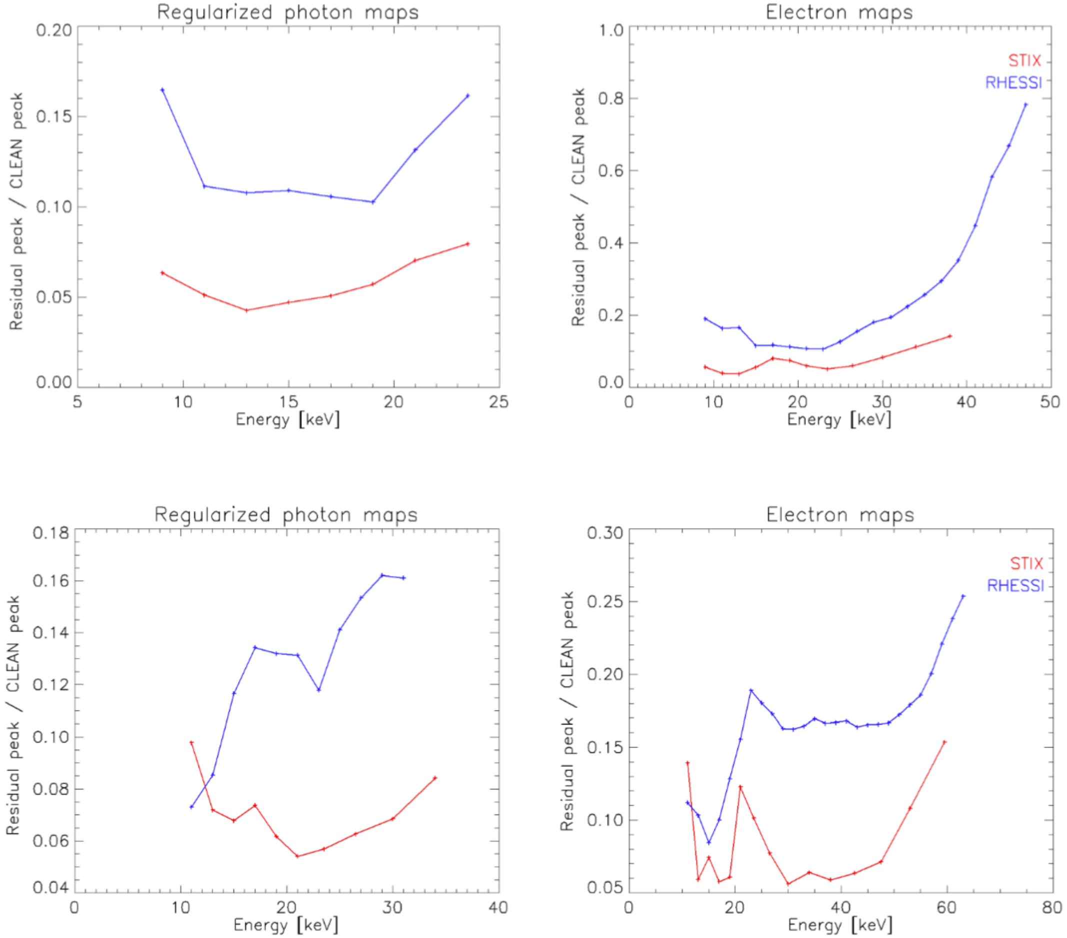

Figure: Ratio between the maximum of the residual map and the maximum of the Clean map at different energies. Red: STIX; blue: RHESSI. *Top row*: Comparison between January 11, 2023 event (STIX) and December 02, 2003 event (RHESSI). *Bottom row*: Comparison between November 11, 2022 event (STIX) and February 20, 2002 event (RHESSI)

Outline

1. From photon to electron visibilities
2. Visibility inversion algorithm
3. Application to STIX visibilities
4. **Conclusions and future works**

Conclusions and future works

- ☑ We have described an approach to solar hard X-ray imaging spectroscopy:
  - ☑ two-dimensional Fourier transforms of the image in the photon domain are transformed into Fourier transforms of the electron flux maps.
  - ☑ This tool also provides regularized photon visibilities corresponding to the regularized electron visibilities.

Conclusions and future works

- ☑ We have described an approach to solar hard X-ray imaging spectroscopy:
  - ☑ two-dimensional Fourier transforms of the image in the photon domain are transformed into Fourier transforms of the electron flux maps.
  - ☑ This tool also provides regularized photon visibilities corresponding to the regularized electron visibilities.

- ☑ We have shown that STIX inversion software seem to work better than RHESSI inversion software.
  - ☐ We are working to investigate why.

Conclusions and future works

- ☑ We have described an approach to solar hard X-ray imaging spectroscopy:
    - ☑ two-dimensional Fourier transforms of the image in the photon domain are transformed into Fourier transforms of the electron flux maps.
    - ☑ This tool also provides regularized photon visibilities corresponding to the regularized electron visibilities.

- ☑ We have shown that STIX inversion software seem to work better than RHESSI inversion software.
    - ❑ We are working to investigate why.

- ❑ We are working on electron spectra for analizing the electron transport effects.

- ❑ We are working to obtain:
    - the average density along the line of sight;
    - number spectrum of accelerated electrons.

THANK YOU FOR THE ATTENTION!

volpara@dima.unige.it

Università di Genova
DIMA | Dipartimento di Matematica
MIDA group